

# On the Causality of Dynamical Systems

Thomas C. Fraser<sup>1,2</sup>

<sup>1</sup>Perimeter Institute for Theoretical Physics, Waterloo, Ontario, Canada, N2L 2Y5

<sup>2</sup>Dept. of Physics and Astronomy, University of Waterloo, Waterloo, Ontario, Canada, N2L 3G1

November 15, 2019

## Comments

These notes can be found at [https://github.com/tcfraser/pearl\\_and\\_dynamic\\_causality](https://github.com/tcfraser/pearl_and_dynamic_causality).

## 1 Overview

### 1. Origins in early chaos theory

- Lorenz's system (Lorenz 1963)
- Attractors
- Reconstructing attractors (Packard et al. 1980)
- Takens' Theorem (Takens 1981)

### 2. Techniques for Dynamical causal discovery

- Convergent Cross-mapping (CCM) (Sugihara et al. 2012)
- Topological Causality (TC) (Harnack et al. 2017)
- Dimensional Causality (DC) (Benkő et al. 2018)

The **dynamical systems** which will be considered here involved a finite number  $n$  of variables  $\{X_1, X_2, \dots, X_n\}$  evolving according to a system of deterministic, first-order, time-independent, ordinary differential equations (discrete or continuous in time).

$$\frac{dX_j}{dt} = f_j(X_1(t), X_2(t), \dots, X_n(t))$$

The solution to a dynamical system on a manifold  $M$  (for example  $\mathbb{R}^n$ ) is specified by a **flow**

$$\Phi_{(\cdot)}(\cdot) : \mathbb{R} \times M \rightarrow M, \tag{1}$$

where  $\Phi_t$  is a diffeomorphism of  $M$  for all  $t \in \mathbb{R}$  such that

$$\forall V \in M : \Phi_0(V) = V, \quad \text{and} \quad \forall s, t \in \mathbb{R} : \Phi_t \circ \Phi_s = \Phi_{s+t}. \tag{2}$$

## 2 A Chaotic Origin Story

### 2.1 Lorenz's Discovery

In “Deterministic nonperiodic flow” (Lorenz 1963), Lorenz (this is Edward Norton Lorenz, not to be confused with the physicist Ludvig Lorenz, or the actor Edward Norton) presented a simplified dynamical model for atmospheric convection, which today is known as the Lorenz system:

$$\begin{aligned}\frac{dX}{dt} &= \sigma(Y - X), \\ \frac{dY}{dt} &= X(\rho - Z) - Y, \\ \frac{dZ}{dt} &= XY - \beta Z.\end{aligned}\tag{3}$$

The Lorenz system was remarkable because despite its determinism and simplicity, it exhibits flows which are non-periodic, chaotic and yet bounded as in Figure 1. Moreover, Lorenz identifies the non-linearity of the equations as being essential for these features postulates their ubiquity.

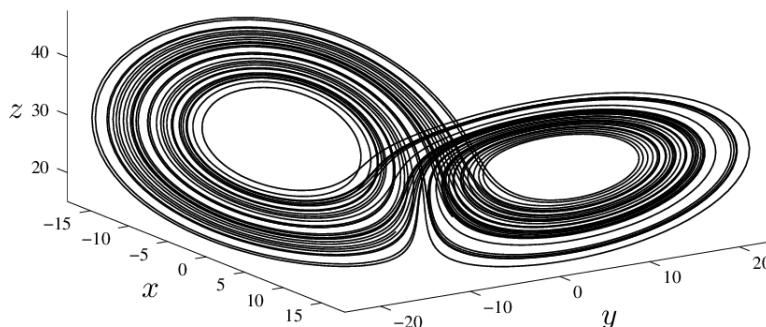


Figure 1: The strange attractor of the Lorenz system for  $\sigma = 10, \beta = 8/3, \rho = 28$  with  $X(0) = 1.1, Y(0) = -1.9, Z(0) = 13.1$ . Figure by P. T. Clemson.

Later in “On the nature of turbulence” (Ruelle and Takens 1971), Ruelle and Takens develop a variety of mathematics to study such quasi-periodic behaviors and refers to them as *strange attractors*. Importantly, they conjectured that universally, strange attractors were the cause of turbulent behaviors seen in fluid flow. This conjecture received further support after “Onset of turbulence in a rotating fluid” (Gollub and Swinney 1975).

### 2.2 What are attractors anyway?

What exactly is notion of an *attractor*? Intuitively, attractors generalize the more familiar notions of stability for differential equations such as *stable fixed points* and *limit cycles* in the sense that an attractor  $A$  is a compact subset such that points starting sufficiently close to  $A$  will remain in a given neighborhood of  $A$ . For a detailed account of the various notions and formulations of an attractor, see “On the concept of attractor” (Milnor 1985). Nevertheless, the following definition will be adequate.

An **attractor** is any  $A \subseteq M$  which is

1. forward invariant

$$\forall a \in A, \forall t \geq 0 : \Phi_t(a) \in A,$$

2. admits an neighborhood  $B(A)$ , called the **basin of attraction**, such for every open neighborhood  $N$  of  $A$ , there is a sufficiently large  $T$  such that

$$\forall b \in B(A), \forall t \geq T : \Phi_t(b) \in N,$$

3. and finally, there is no other proper subset  $A' \subset A$  satisfying the above.

Note that some alternative definitions demand that  $A$  has non-zero measure (i.e. to eliminate stable fixed points) or that there exists a orbit of the flow that is dense inside  $A$ .

What makes a strange attractor so *strange*? At the time, Ruelle and Takens never articulated a concrete definition for strange attractors, instead it was simply an attractor that was “strange” to them. Today, strange attractors are defined to be attractors whose dimension is not an integer, i.e. a fractal. Of course, the Lorenz attractor is a strange attractor in this sense as well, as proven in “A rigorous ODE solver and Smale’s 14th problem” (Tucker 2002).

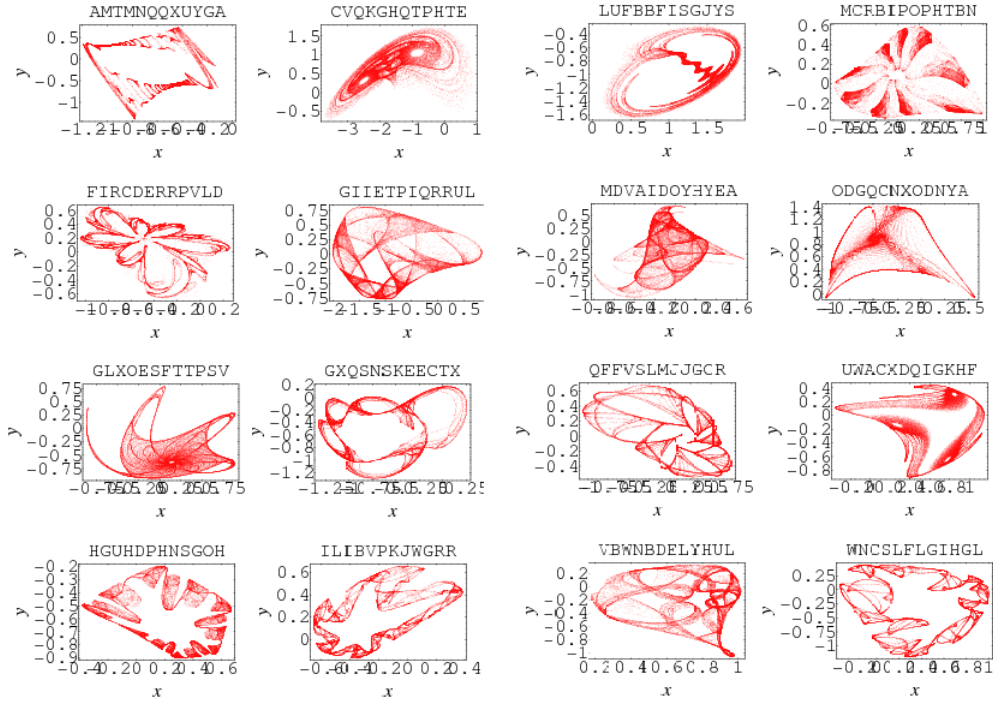


Figure 2: Some strange attractors. Figures from E. W. Weisstein.

## 2.3 Reconstructing Attractors

In “Geometry from a time series” (Packard et al. 1980), Packard et al. were interested in problem of *dynamical reconstruction*: from experimental observations of a turbulent fluid flow, how does one show the existence of a low-dimensional chaotic dynamical system which explains the observed behaviors? Additionally, how does one determine the dimensionality of the underlying attractor? They demonstrate their ideas using another non-linear dynamical system studied by (Rössler 1976):

$$\begin{aligned}
\frac{dX}{dt} &= -(Y + Z), \\
\frac{dY}{dt} &= X + 0.2Y, \\
\frac{dZ}{dt} &= 0.4 + XZ - 5.7Z.
\end{aligned} \tag{4}$$

Their reconstruction method relied directly on the intuition that in order to specify the state of an  $n$ -dimensional system at any given time, it is sufficient to know the values of *any* set of  $n$  “independent” quantities. Moreover, they conjecture that the attractors associated with any such are all *diffeomorphically* equivalent. To support this claim, they compare various trajectories in 3-dimensions of the Rossler system:  $\{X(t), Y(t), Z(t)\}$ ,  $\{X(t), X(t - \tau), X(t - 2\tau)\}$  (this example is credited to Ruelle by the authors), and  $\{X(t), \dot{X}(t), \ddot{X}(t)\}$  (by making  $\tau$  very small and taking appropriate differences).

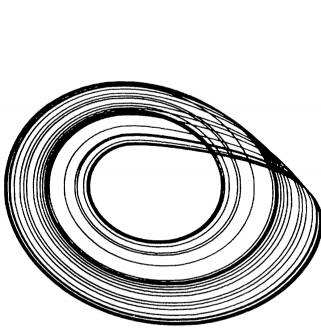


FIG. 1.  $(x, y)$  projection of Rossler (Ref. 7).

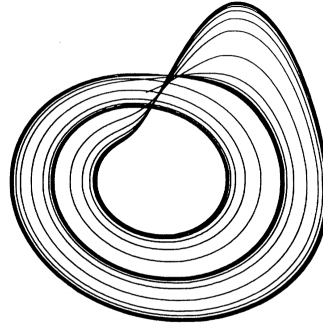


FIG. 2.  $(x, \dot{x})$  reconstruction from the time series.

Figure 3: The Rössler system flow projected onto the  $X, Y$  plane and the induced flow of  $(X, \dot{X}, \ddot{X})$  projected onto the  $X, \dot{X}$  plane. Figure from (Packard et al. 1980).

Evidently their heuristic seems to work and moreover it appears possible to reconstruct the dynamics from observing just a single coordinate. They further provide some tools for estimating the dimensionality of the attractor and how it relates to the number non-negative characteristic exponents.

## 2.4 Takens’ Theorem

Shortly after this, in “Detecting strange attractors in turbulence” (Takens 1981), Takens formalized and proved the conjecture of (Packard et al. 1980) which has come to be known as *Takens’ Theorem*. The following is a summary of [Marco Vitturi’s slides](#) on the subject.

**Whitney Embedding Theorem:** Let  $M$  be a compact manifold of (integer) dimension  $d$ . Then  $M$  can be embedded smoothly in  $\mathbb{R}^{2d}$  (i.e. no self-intersections).

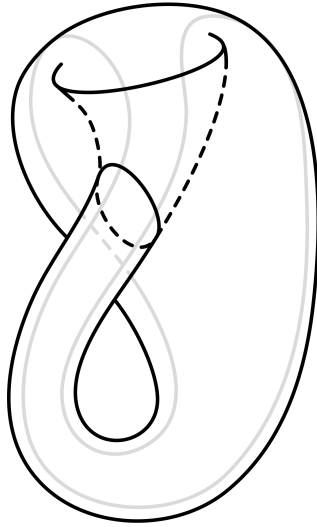


Figure 4: The Klein bottle can be embedded smoothly in  $\mathbb{R}^4$ , but not in  $\mathbb{R}^3$ .

**Takens' Theorem:** Let  $M$  be a compact manifold of (integer) dimension  $d$ . Then for *generic* pairs  $(\phi, X)$ , where

- $\phi : M \rightarrow M$  is a  $C^2$ -diffeomorphism of  $M$  in itself,
- $X : M \rightarrow \mathbb{R}$  is a  $C^2$ -differentiable function,

then the map  $\Omega_{\phi, X} : M \rightarrow \mathbb{R}^{2d+1}$  acting on  $V \in M$  defined by

$$\Omega_{\phi, X}(V) = (X(V), X(\phi(V)), X(\phi^2(V)), \dots, X(\phi^{2d}(V)))$$

is an embedding of  $M$  into  $\mathbb{R}^{2d+1}$  (i.e. injective and immersive).

Takens' theorem when applied to the flow of a dynamical system in  $\mathbb{R}^n$  when  $M$  is taken to be the attractor (assume manifold)  $A$ :

- $\phi = \Phi_{-\tau} : A \rightarrow A$  for some  $\tau > 0$ ,
- $X : A \rightarrow \mathbb{R}$  any coordinate of the system on the attractor,
- the **delay embedding** becomes

$$\begin{aligned} \Omega_{\Phi_{-\tau}, X}(V) &= (X(V), X(\Phi_{-\tau}(V)), X(\Phi_{-2\tau}(V)), \dots, X(\Phi_{-m\tau}(V))) \\ &= (X(t), X(t - \tau), X(t - 2\tau), \dots, X(t - m\tau)) \end{aligned}$$

- where  $m$  needs to be sufficiently large, i.e.  $m \geq 2\dim(A)$  is sufficient.
- Oftentimes a smaller  $m$  will still produce an embedding, but Takens' theorem does not guarantee this.

A similar result can be stated for reconstructing the orbit in  $\mathbb{R}^d$  instead of the entire attractor, you can use  $m = d - 1$ . Therefore a single variable contains all the information about the orbit:

$$t \mapsto (X(t), X(t - \tau), X(t - 2\tau), \dots, X(t - (d - 1)\tau)).$$

An analogous version for the case of non-integer (Hausdorff) dimensions  $d_A$  is due to “Embedology” (Sauer, Yorke, and Casdagli 1991), where  $m \geq \lceil 2d_A \rceil$ .

Therefore, the attractor  $A$  of the original system is diffeomorphic to the time-delayed attractors  $A_X, A_Y$  and  $A_Z$  where  $A_X = \Omega_{\Phi_{-\tau}, X}(A)$ .

Evidently, Takens’ theorem reveals that the distinction between the kinematics and dynamics of a system is an arbitrary distinction as one can freely transform between the various phase-spaces in a diffeomorphic way. For similar instances of this arbitrary distinction, and more ideas on this subject, see “The paradigm of kinematics and dynamics must yield to causal structure” (Spekkens 2015).

## 3 Selected References on Dynamic Causality

### 3.1 Granger Causality

There is a pervasive notion of causality used frequently in economic forecasting, but also in neurology and ecology, known as *Granger Causality* or sometimes *G-Causality* named after Clive Granger. For evidence, the library of software tools “The MVGC multivariate Granger causality toolbox: a new approach to Granger-causal inference” (Barnett and Seth 2014) is highly cited. Its origins can be traced back to a suggestion due to (Wiener, 1956) for using prediction as a proxy for causality, which was subsequently developed by Granger from 1963 to 1980. Granger was awarded the Nobel Prize in Economics in 2003.

In “Some recent development in a concept of causality” (Granger 1988), Granger summarizes his notions of causality for time-series’ which were based on two principles:

1. The cause occurs before the effect.
2. The causal series (say  $Y(t)$ ) contains *special information* about the series being caused (say  $X(t)$ ) that is not available in the any other available series (say  $W(t)$ ).

Consider two sets of historical data:

$$J_t = \{(X(t-j), Y(t-j), W(t-j)) | j \geq 0\} \quad (5)$$

$$J'_t = \{(X(t-j), W(t-j)) | j \geq 0\}. \quad (6)$$

His definitions pertain to the following: in the context of  $W$ , does  $Y$  cause  $X$ ?

Letting  $P(X|J)$  denote the conditional distribution of  $X$  given  $J$ , if  $P(X(t+1)|J_t) = P(X(t+1)|J'_t)$  then  $Y(t)$  does *not cause*  $X(t)$ , otherwise  $Y(t)$  is a *prima facie cause* of  $X(t)$  and becomes a cause with certainty is  $J_t$  contains all the information in the universe. Granger acknowledges a number of criticisms in his works.

Most relevant for the current discussion is the article “Inferring connectivity in networked dynamical systems: Challenges using Granger causality” (Lusch, Maia, and Kutz 2016), which simulated network systems of Kuramoto oscillators and then used the MGVC toolbox to reconstruct the network structure. They write “Our results show a significant systematic disparity between the original and inferred network, unless the true structure is extremely sparse or dense.”

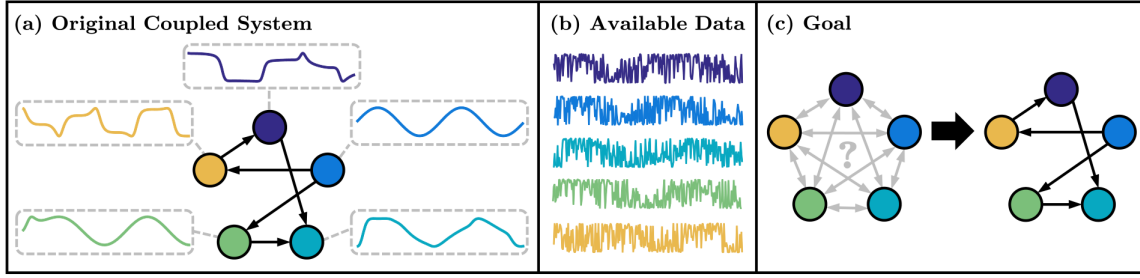


FIG. 1. Inferring network connectivity via Granger causality analysis. (a) Schematics of a coupled dynamical system where the directed network architecture plays an important role. The time series generated by each node is influenced by its connectivity to other nodes. (b) In several applications, the connectivity structure is unknown, but noisy measurements from each node are available. (c) We use Granger causality to infer the original network structure from the noisy data.

Figure 5: The methodology used by “Inferring connectivity in networked dynamical systems: Challenges using Granger causality” (Lusch, Maia, and Kutz 2016).

Clearly, Granger’s notions of causality are inappropriate for the purposes of causal modeling, despite its widespread use.

### 3.2 Convergent Cross Mapping (CCM)

The seminal article titled “Detecting causality in complex ecosystems” (Sugihara et al. 2012) has been widely cited in other articles on dynamical causality and throughout ecological and economic communities. Its essential accomplishment, in my opinion, was the realization that nonlinear dynamical systems exhibit a kind of nonseparability which must be dealt with first in order analyze the underlying causal relations and moreover that Takens’ theorem resolves this nonseparability.

It opens with an discussion around the notions of ephemeral or “mirage” correlations. The following discrete-time non-linear dynamical system,

$$\begin{aligned} X(t+1) &= X(t)(r_x - r_x X(t) - \beta_{x,y} Y(t)) \\ Y(t+1) &= Y(t)(r_y - r_y Y(t) - \beta_{y,x} X(t)) \end{aligned} \tag{7}$$

exhibits periods of correlation, anticorrelation and no correlation.



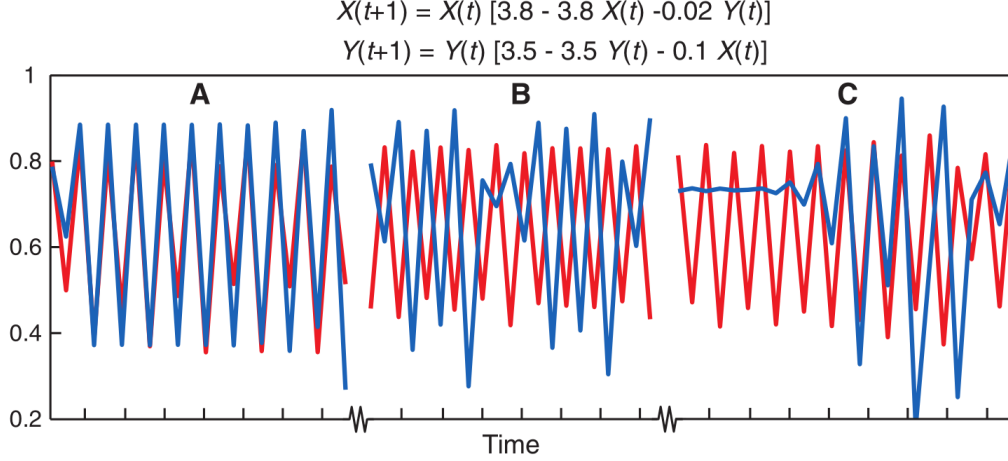


**Fig. 1.** Mirage correlations. (A to C) Three samples from a single run of a coupled two-species nonlinear logistic difference system with chaotic dynamics. Variables  $X$  (blue) and  $Y$  (red) appear correlated in the first time segment (A), anticorrelated in the second time segment (B), and lose all coherence in the third time segment (C) with alternating interspersed periods of positive, negative, and zero correlation. Although the system is deterministic and dynamically coupled, there is no long-term correlation ( $n = 1000$ ,  $\rho = 0.0054$ ,  $P = 0.864$ ).

Figure 6: An illustration of mirage correlations from “Detecting causality in complex ecosystems” (Sugihara et al. 2012).

Therefore, using correlation to infer causation is risky, especially in nonlinear dynamics. Moreover, this demonstrates why a lack of correlation does not imply a lack of causation because the former could simply be temporary. In other words, the principle of no fine-tuning only applies in the long term.

Sugihara et al. attributes the inadequacy of Granger causality for dynamical systems to Takens’ theorem. In particular, “information about  $X(t)$  that is relevant to predicting  $Y$  is redundant in this system”. Stated another way, by algebraically rearranging Eq. 7, it is possible to write  $Y(t+1)$  in terms of  $Y(t)$  and  $Y(t-1)$ ; thus Granger causality predicts  $X$  does not cause  $Y$ ! In “Topological causality in dynamical systems” (Harnack et al. 2017), this nonseparability is referred to as an *entanglement* between  $X$  and  $Y$ .

The essential idea of (Sugihara et al. 2012) is that time-series variables  $X$  and  $Y$  are *causally linked* if they share a common attractor manifold  $A$ ; therefore, each variable can identify the other. Convergent cross mapping (CCM) tests for causal influence from  $X$  to  $Y$  by measuring the extent to which the history of  $Y$  can reliably estimate the states of  $X$ . For example, a fish time series  $Y$  can be used to estimate the weather  $X$ , but not conversely, thus  $X$  causes  $Y$ ; this is counter to Granger causality.



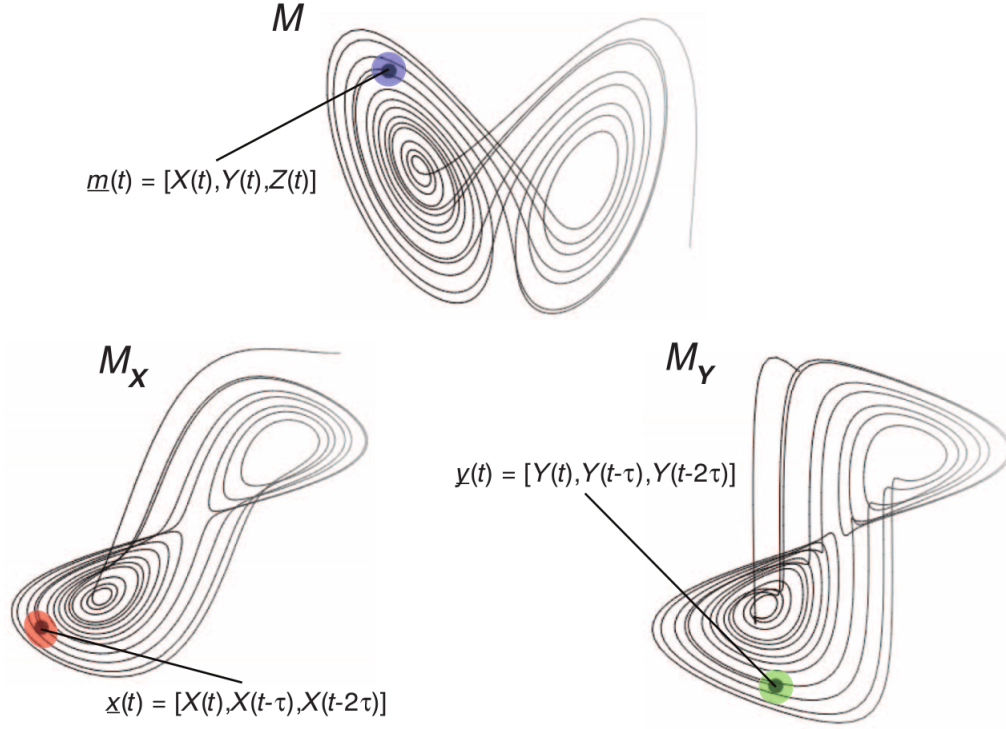


**Fig. 2.** Convergent cross mapping (CCM) tests for correspondence between shadow manifolds. This example based on the canonical Lorenz system (a coupled system in  $X$ ,  $Y$ , and  $Z$ ; eq. S7 without  $V$ ) shows the attractor manifold for the original system ( $M$ ) and two shadow manifolds,  $M_X$  and  $M_Y$ , constructed using lagged-coordinate embeddings of  $X$  and  $Y$ , respectively (lag =  $\tau$ ). Because  $X$  and  $Y$  are dynamically coupled, points that are nearby on  $M_X$  (e.g., within the red ellipse) will correspond temporally to points that are nearby on  $M_Y$  (e.g., within the green circle). That is, the points inside the red ellipse and green circle will have corresponding time indices (values for  $t$ ). This enables us to estimate states across manifolds using  $Y$  to estimate the state of  $X$  and vice versa using nearest neighbors (3). With longer time series, the shadow manifolds become denser and the neighborhoods (ellipses of nearest neighbors) shrink, allowing more precise cross-map estimates (see movies S1 to S3).

Figure 7: The method of convergent cross mapping (CCM) due to “Detecting causality in complex ecosystems” (Sugihara et al. 2012).

### Sketching the CCM Algorithm:

1. Given two time series of length  $L$ ,

$$\{X(1), X(2), \dots, X(L)\} \quad \text{and} \quad \{Y(1), Y(2), \dots, Y(L)\},$$

here is how to estimate  $Y(t)$  using  $X$ .

2. Compute the time lagged coordinate

$$\underline{X}(t) = (X(t), X(t - \tau), X(t - 2\tau), \dots, X(t - (d - 1)\tau)).$$

3. Then find its  $d + 1$  nearest neighbors in  $A_X$ , denoted

$$(\underline{X}(t_1), \underline{X}(t_2), \dots, \underline{X}(t_{d+1})),$$

thus forming a  $d$ -dimensional simplex around  $\underline{X}(t)$ .

4. Construct the estimate  $\hat{Y}(t)$  for  $Y(t)$  as

$$\hat{Y}(t)|A_X = \sum_{i=1}^{d+1} \omega_i Y(t_i)$$

where the weight  $\omega_i$  is based on the distance between  $\underline{X}(t)$  and  $\underline{X}(t_i)$ .

5. As the length  $L$  increases, the attractor manifold is filled in more and more, and the nearest neighbors get closer and thus  $\hat{Y}(t)|A_X$  should converge to  $Y(t)$  (if  $Y$  has causal influence on  $X$ ) and vice versa.

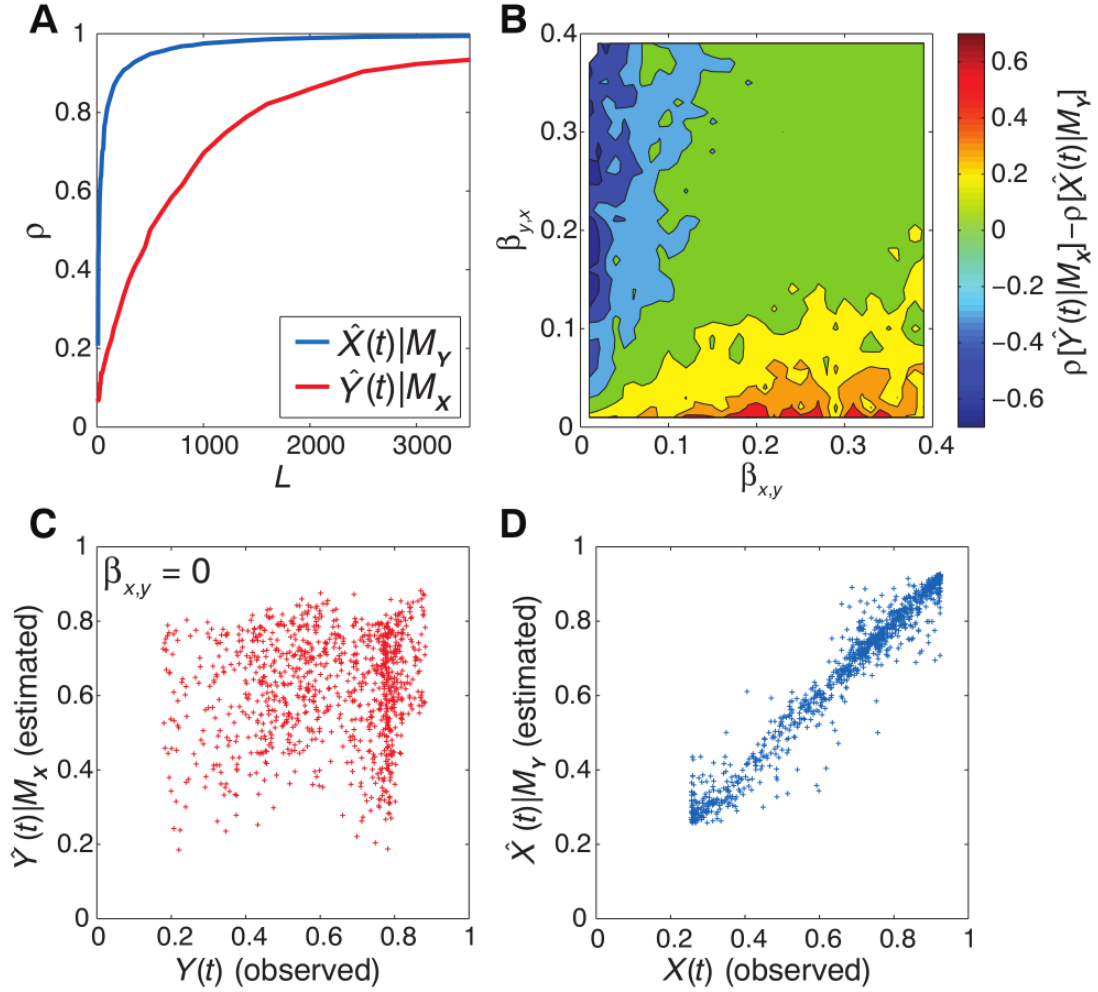
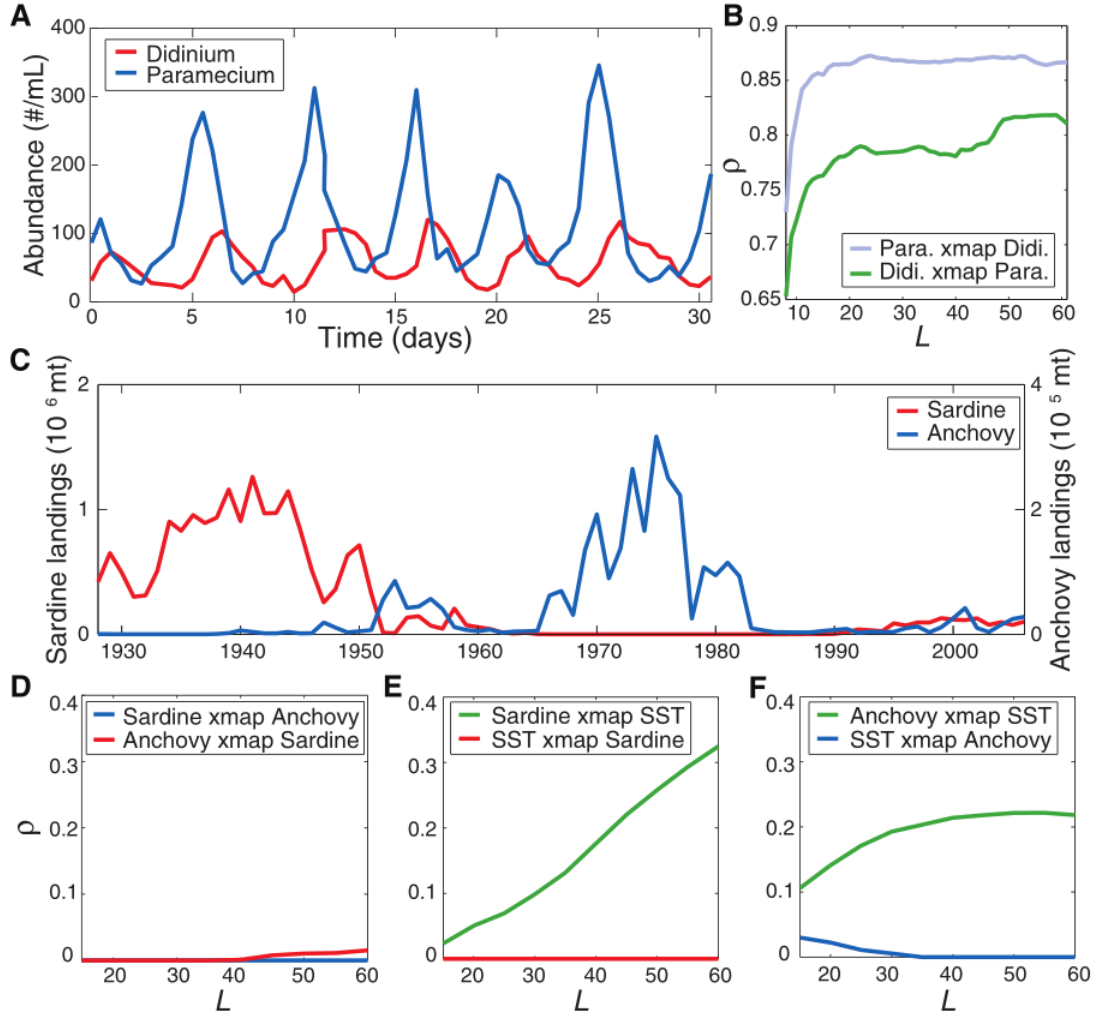


Figure 8: Empirical results for CCM on Eq. 7. (A) CCM where  $\beta_{y,x} > \beta_{x,y}$ ; the asymmetry is reflected in the differing rates of convergence. (B) How the difference in cross-mapping estimates depends on  $\beta_{x,y}$  and  $\beta_{y,x}$ . (C,D) Estimates when  $\beta_{x,y} = 0$ , i.e. when  $Y$  has no effect on  $X$ . From “Detecting causality in complex ecosystems” (Sugihara et al. 2012).



**Fig. 5.** Detecting causation in real time series. **(A)** Abundance time series of *Paramecium aurelia* and *Didinium nasutum* as reported in (28). **(B)** CCM of *Paramecium* and *Didinium* with increasing time-series length  $L$ . The pattern suggests top-down predator control. **(C)** California landings of Pacific sardine (*Sardinops sagax*) and northern anchovy (*Engraulis mordax*). **(D to F)** CCM (or lack thereof) of sardine versus anchovy, sardine versus SST (Scripps Pier), and anchovy versus SST (Newport Pier), respectively. This shows that sardines and anchovies do not interact with each other and that both are forced by temperature.

Figure 9: (C-F) CCM resolves a long-disputed causal relationship between populations of sardines and anchovies along with sea surface temperatures (SST) measured at Scripps Pier and Newport Pier in California; sardines and anchovies are not interacting, but share a common cause, namely SST. From “Detecting causality in complex ecosystems” (Sugihara et al. 2012).

Future work demonstrated that CCM successfully distinguishes between direct and indirect causation in causal chains (Ye et al. 2015).

### 3.3 Topological Causality (TC)

In “Topological causality in dynamical systems” (Harnack et al. 2017), the concepts of CCM are expanded upon further.

$$\begin{aligned}\frac{dX_1}{dt} &= f_1(X_1, w_{12}\mu_2(X_2)) \\ \frac{dX_2}{dt} &= f_2(X_2, w_{21}\mu_1(X_1))\end{aligned}$$

Theoretically, if the diffeomorphism between the attractor manifolds is differentiable, then it can be linearized at a fixed time  $t$  (Jacobian matrix), denoted  $M_{i \rightarrow j}^t$ . The *expansion* of this linear map, denoted

$$e_{i \rightarrow j}^t = \prod_k \max(1, \sigma_k(M_{i \rightarrow j}^t))$$

is conjectured to be inversely proportional to the strength of the causal influence  $X_j \rightarrow X_i$  ( $\sigma_k(M_{i \rightarrow j}^t)$  is the  $k$ -th singular value of  $M_{i \rightarrow j}^t$ ). Unlike vanilla CCM, TC computes a *graduated* measure causal influence which furthermore can be taken to be time-dependent.

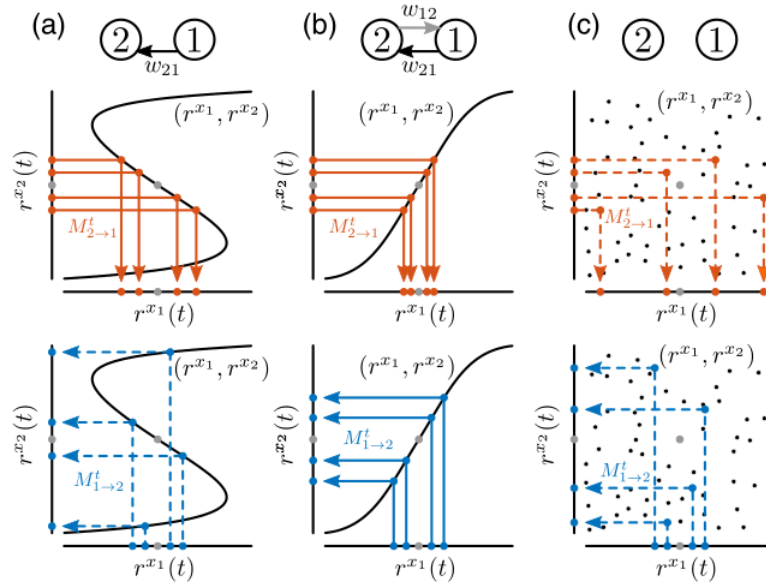


FIG. 1. The relation of points  $\mathbf{r}^{x_1}$  and  $\mathbf{r}^{x_2}$  on multidimensional manifolds illustrated in one dimension. The joint manifold represented by  $(\mathbf{r}^{x_1}, \mathbf{r}^{x_2})$  can be interpreted as the function mediating the mappings  $M_{i \rightarrow j}$  between both spaces, and local linearizations  $M_{i \rightarrow j}^t$  of the mappings as the slope around a reference point. (a) When only  $w_{21} \neq 0$ , a one-to-one mapping  $M_{2 \rightarrow 1}$  from  $\mathbf{r}^{x_2}$  to  $\mathbf{r}^{x_1}$  exists, but not in the reverse direction:  $\mathbf{r}^{x_2}(t)$  is not uniquely determined for all states  $\mathbf{r}^{x_1}(t)$ . Locally,  $M_{1 \rightarrow 2}^t$  can be attributed a diverging expansion property, since close neighbors of a given point  $\mathbf{r}^{x_1}(t)$  correspond to distant parts of the joint density  $(\mathbf{r}^{x_1}, \mathbf{r}^{x_2})$ . The dashed lines visualize nonuniqueness. (b) Here, both couplings are nonzero, but  $w_{21} > w_{12}$ . Larger independence of  $x_1$  implies a stronger expansion by  $M_{1 \rightarrow 2}^t$  than by  $M_{2 \rightarrow 1}^t$  at most reference points, which is indicated by the higher slope of  $(\mathbf{r}^{x_1}, \mathbf{r}^{x_2})$  when seen from  $\mathbf{r}^{x_1}$ . (c) If no coupling exists, expansion diverges in both directions.

Figure 10: The intuition behind the inverse relationship between expansion and causal influence in “Topological causality in dynamical systems” (Harnack et al. 2017).

### 3.4 Dimensional Causality (DC)

The latest development in the field of dynamic causality based on Takens’ theorem is the article “Exact Inference of Causal Relations in Dynamical Systems” (Benkő et al. 2018), which presents a method called *Dimensional Causality* (DC). While recognizing the utility of the CCM (Sugihara et al. 2012) and TC (Harnack et al. 2017) techniques for detecting directed and bidirected causal relationships, Benkő et al. identifies their inability to consistently and accurately identify latent common causes. To their best knowledge, “the DC method is the first exact one which detects and distinguishes all possible causal relations of deterministic dynamical systems.”

The entire technique heavily relies on the ability to estimate the manifold of an attractor from observational data; the authors use the method in “Manifold-adaptive dimension estima-

tion” (Szepesvári, Audibert, et al. 2007) which depends only on a single parameter  $k$  related to the resolution.

In order to detect the causal structure underlying two variables  $X, Y$ , there are three attractor manifolds of interest  $A_X, A_Y$  and  $A_J$  where  $J = X \times Y$  is the joint system. In practice however, they construct the joint dynamics additively using  $J' = aX + Y$  with suitably chosen irrational number (they use  $a = \sqrt{29/31}$  as its close to unity).

If the two variables are independent, the joint dimension will equal the sum of the dimensions of the independent systems.

$$\text{Independent case: } X \perp Y \iff D_X + D_Y = D_J$$

Any interdependence between  $X$  and  $Y$  will lead to subadditivity in the manifold dimensions. Whenever there is unidirectional causation  $X \rightarrow Y$ , the information content in the consequent  $Y$  is capable of determining the cause  $X$ , therefore the dimensions  $D_X, D_Y$  unequivocally determine the direction of possible causal effect (see Figure 11 (A)),

$$\text{Unidirectional case: } X \rightarrow Y \iff D_X < D_Y = D_J$$

The bidirected case follows naturally, as Takens’ theorem proves  $A_X$  and  $A_Y$  are topologically equivalent and thus have the same dimension.

$$\text{Bidirectional case: } X \leftrightarrow Y \iff D_X = D_Y = D_J$$

Detecting the presence of a common cause (without direct causal effect between  $X$  and  $Y$ ) is trickier to motivate.

$$\text{Common cause case: } X \nwarrow \nearrow Y \iff \max(D_X, D_Y) < D_J < D_X + D_Y$$

Alternatively, these relationships become clearer when you realize that the authors are using the Rényi information dimension to estimate the dimensions of the attractors:

$$d_X = \lim_{N \rightarrow \infty} \frac{1}{\log N} H([X]_N)$$

where  $H$  is the Shannon entropy and  $[X]_N = \lfloor NX \rfloor / N$  is the  $N$ -quantized discrete version of  $X$ . Elementary entropic inequalities give

$$\max(H(X), H(Y)) \leq H(X, Y) \leq H(X) + H(Y),$$

which translates to the common cause condition above.

To showcase their method, they consider the logistic map,

$$X_j[t+1] = rX_j[t](1 - \sum_{l=1}^3 \beta_{jl} X_l[t])$$

with  $j, l \in \{1, 2, 3\}$  and  $r = 3.99$ . The various causal scenarios are implemented as follows:

$$\beta_{\rightarrow} = \begin{bmatrix} 1 & 0 & 0 \\ 0.5 & 1 & 0 \\ 0 & 0 & 1 \end{bmatrix} \quad \beta_{\leftrightarrow} = \begin{bmatrix} 1 & 0.5 & 0 \\ 0.5 & 1 & 0 \\ 0 & 0 & 1 \end{bmatrix} \quad \beta_{\nwarrow \nearrow} = \begin{bmatrix} 1 & 0 & 0.5 \\ 0 & 1 & 0.5 \\ 0 & 0 & 1 \end{bmatrix} \quad \beta_{\perp} = \begin{bmatrix} 1 & 0 & 0 \\ 0 & 1 & 0 \\ 0 & 0 & 1 \end{bmatrix}$$

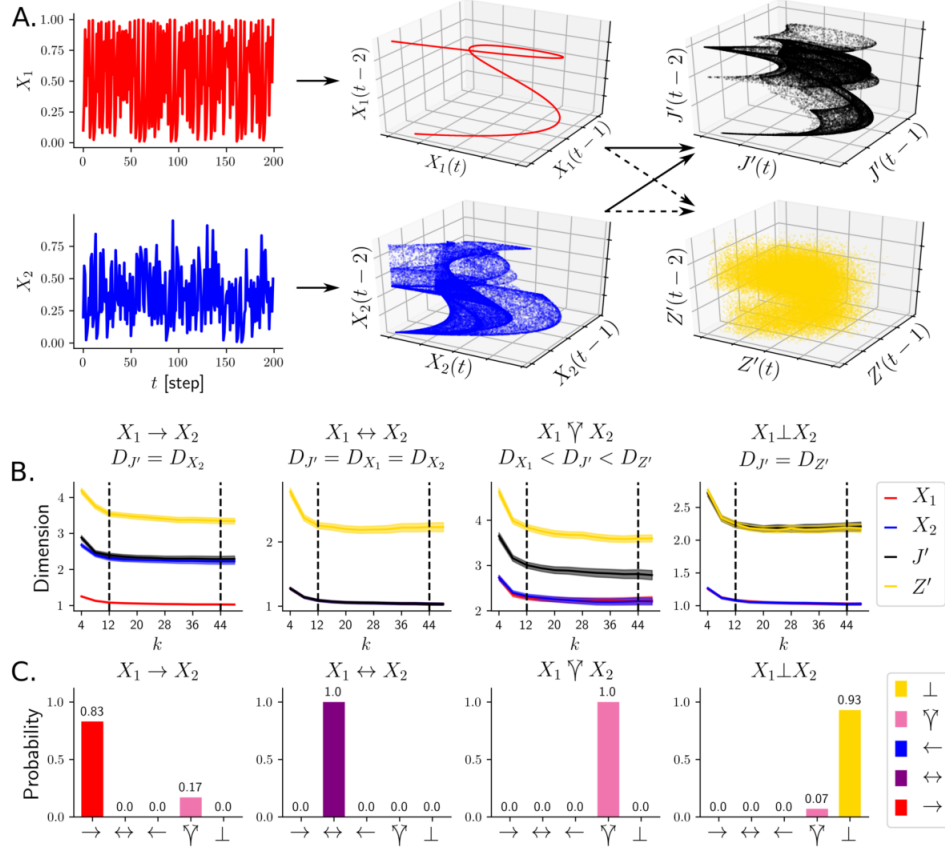


Figure 1: *The workflow and testing of the Dimensional Causality method on coupled logistic map systems (see Eq. 5). (A) The state spaces of the systems are reconstructed by time delay embedding of the two time series  $X_1$  (red)*

Figure 11: Dimensional Causality identifies a variety of causal structures. From “Exact Inference of Causal Relations in Dynamical Systems” (Benkő et al. 2018).

The also demonstrate their method on empirically obtained data and get interesting results. See scanned notes for more comments.



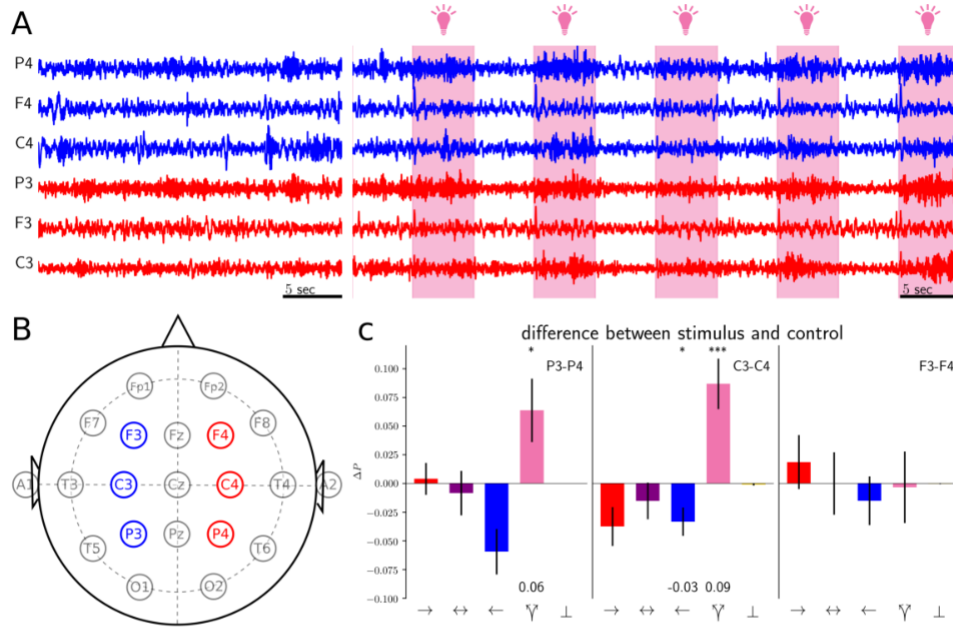


Figure 4: *Inter-hemispherical interactions during photo-stimulation.* (A) CSD signal in control condition and photo-stimulation periods (light bulbs) at the six analyzed recording-channels and (B) electrode positions on the scalp. Causal relations were computed between P3-P4, C3-C4 and F3-F4 channel pairs. (C) Difference in probabilities of causal relations between stimulation and control (mean and SE). The probability of the existence of common cause is significantly higher during stimulation periods for P3-P4 ( $p = 0.024$ ) and C3-C4 ( $p = 0.0002$ ) channel-pairs but not for F3-F4 ( $n = 87$ ).

Figure 12: An application of the technique of dimensional causality in “Exact Inference of Causal Relations in Dynamical Systems” (Benkő et al. 2018).

## 4 Other Noteworthy Articles

In “Causality in complex systems” (Wagner 1999), Wagner argues that a “...notion of causality can only be meaningfully defined for systems with *linear* interactions among their variables. For the vastly more important class of *nonlinear* systems, no such notion is likely to exist.”

In “Linking granger causality and the pearl causal model with settable systems” (White, Chalak, and Lu 2011), White, Chalak, and Lu use the formalism of *settable systems*, a generalization of Pearl’s Causal Models (Pearl 2000), to closely link the concepts of Granger causality to that of Pearl causality.

At a quick glance, “Beyond Structural Causal Models: Causal Constraints Models” (Blom, Bongers, and Mooij 2019) appears to be doing a similar thing but for systems at a stable fixed point.

Also “Dynamic causality in event structures” (Arbach et al. 2015).

## References

- Allen, John-Mark A et al. (2017). “Quantum common causes and quantum causal models”. In: *Physical Review X* 7.3, p. 031021.
- Arbach, Youssef et al. (2015). “Dynamic causality in event structures”. In: *International Conference on Formal Techniques for Distributed Objects, Components, and Systems*. Springer, pp. 83–97.
- Barnett, Lionel and Anil K Seth (2014). “The MVGC multivariate Granger causality toolbox: a new approach to Granger-causal inference”. In: *Journal of neuroscience methods* 223, pp. 50–68.
- Benkő, Zsigmond et al. (2018). “Exact Inference of Causal Relations in Dynamical Systems”. In: *arXiv preprint arXiv:1808.10806*.
- Blom, Tineke, Stephan Bongers, and Joris M Mooij (2019). “Beyond Structural Causal Models: Causal Constraints Models”. In: *Proceedings of the Conference on Uncertainty in Artificial Intelligence*.
- Boltt, Erik M, Jie Sun, and Jakob Runge (2018). “Introduction to Focus Issue: Causation inference and information flow in dynamical systems: Theory and applications”. In: *Chaos: An Interdisciplinary Journal of Nonlinear Science* 28.7, p. 075201.
- Breuer, Heinz-Peter (2004). “Genuine quantum trajectories for non-Markovian processes”. In: *Physical Review A* 70.1, p. 012106.
- Friston, Karl J et al. (2014). “Granger causality revisited”. In: *NeuroImage* 101, pp. 796–808.
- Gollub, Jerry P and Harry L Swinney (1975). “Onset of turbulence in a rotating fluid”. In: *Physical Review Letters* 35.14, p. 927.
- Granger, Clive WJ (1988). “Some recent development in a concept of causality”. In: *Journal of econometrics* 39.1-2, pp. 199–211.
- Harnack, Daniel et al. (2017). “Topological causality in dynamical systems”. In: *Physical review letters* 119.9, p. 098301.
- Lorenz, Edward N (1963). “Deterministic nonperiodic flow”. In: *Journal of the atmospheric sciences* 20.2, pp. 130–141.
- Lusch, Bethany, Pedro D Maia, and J Nathan Kutz (2016). “Inferring connectivity in networked dynamical systems: Challenges using Granger causality”. In: *Physical Review E* 94.3, p. 032220.
- Milnor, John (1985). “On the concept of attractor”. In: *The theory of chaotic attractors*. Springer, pp. 243–264.
- Mogensen, Søren Wengel, Daniel Malinsky, and Niels Richard Hansen (2018). “Causal Learning for Partially Observed Stochastic Dynamical Systems.” In: *UAI*, pp. 350–360.
- Packard, Norman H et al. (1980). “Geometry from a time series”. In: *Physical review letters* 45.9, p. 712.
- Pearl, Judea (2000). *Causality: models, reasoning and inference*. Vol. 29. Springer.
- Pearl, Judea et al. (2009). “Causal inference in statistics: An overview”. In: *Statistics surveys* 3, pp. 96–146.
- Penny, Will D et al. (2004). “Comparing dynamic causal models”. In: *Neuroimage* 22.3, pp. 1157–1172.
- Poole, David and Mark Crowley (2013). “Cyclic causal models with discrete variables: Markov chain equilibrium semantics and sample ordering”. In: *Twenty-Third International Joint Conference on Artificial Intelligence*.
- Rössler, Otto E (1976). “An equation for continuous chaos”. In: *Physics Letters A* 57.5, pp. 397–398.

- Rubenstein, Paul K et al. (2016). “From deterministic ODEs to dynamic structural causal models”. In: *arXiv preprint arXiv:1608.08028*.
- Ruelle, David and Floris Takens (1971). “On the nature of turbulence”. In: *Les rencontres physiciens-mathématiciens de Strasbourg-RCP25* 12, pp. 1–44.
- Sauer, Tim, James A Yorke, and Martin Casdagli (1991). “Embedology”. In: *Journal of statistical Physics* 65.3-4, pp. 579–616.
- Spekkens, Robert W (2015). “The paradigm of kinematics and dynamics must yield to causal structure”. In: *Questioning the Foundations of Physics*. Springer, pp. 5–16.
- Stephan, Klaas Enno et al. (2010). “Ten simple rules for dynamic causal modeling”. In: *Neuroimage* 49.4, pp. 3099–3109.
- Sugihara, George et al. (2012). “Detecting causality in complex ecosystems”. In: *science* 338.6106, pp. 496–500.
- Szepesvári, Csaba, Jean-Yves Audibert, et al. (2007). “Manifold-adaptive dimension estimation”. In: *Proceedings of the 24th international conference on Machine learning*. ACM, pp. 265–272.
- Takens, Floris (1981). “Detecting strange attractors in turbulence”. In: *Dynamical systems and turbulence, Warwick 1980*. Springer, pp. 366–381.
- Tucker, Warwick (2002). “A rigorous ODE solver and Smale’s 14th problem”. In: *Foundations of Computational Mathematics* 2.1, pp. 53–117.
- Wagner, Andreas (1999). “Causality in complex systems”. In: *Biology and Philosophy* 14.1, pp. 83–101.
- White, Halbert, Karim Chalak, and Xun Lu (2011). “Linking granger causality and the pearl causal model with settable systems”. In: *NIPS Mini-Symposium on Causality in Time Series*, pp. 1–29.
- Wood, Christopher J and Robert W Spekkens (2015). “The lesson of causal discovery algorithms for quantum correlations: Causal explanations of Bell-inequality violations require fine-tuning”. In: *New Journal of Physics* 17.3, p. 033002.
- Ye, Hao et al. (2015). “Distinguishing time-delayed causal interactions using convergent cross mapping”. In: *Scientific reports* 5, p. 14750.